Available online at www.sciencedirect.com
SCIENCE DIRECT®
International Journal of Multiphase Flow 30 (2004) 717–734
International Journal of Multiphase Flow
www.elsevier.com/locate/ijmulflow

Saturated flow boiling heat transfer of environmentally acceptable surfactants ☆

G. Hetsroni [a,*], J.L. Zakin [b], M. Gurevich [a], A. Mosyak [a], E. Pogrebnyak [a], R. Rozenblit [a]

[a] *Department of Mechanical Engineering, Technion—Israel Institute of Technology, Haifa 32000, Israel*
[b] *Department of Chemical Engineering, Ohio State University, Columbus, OH 42210, USA*

Received 7 January 2004; received in revised form 13 April 2004

Abstract

Saturated flow boiling of surfactant solutions was studied and compared to that of pure water. The liquid flowed in an annular space between two vertical tubes. The heat was transferred from the inner heated tube to the outer one. A nonionic surfactant, with negligible environmental impact, was used. The surface tension for the water–surfactant system was determined at various temperatures. High-speed photography was used for direct observation of the sequence of events that occur during flow boiling. The heat transfer experiments focused on the saturated boiling regime. Addition of surfactant to water produced a large number of small diameter bubbles, which, at high heat fluxes, tend to cover the entire heater surface with a vapor blanket. Boiling heat transfer coefficients in surfactant solution are higher than that in pure water.

Keywords: Flow boiling; Boiling regimes; Heat transfer; Liquid film evaporation; Surfactants

1. Introduction

Flow boiling heat transfer of Newtonian fluids has been studied extensively due to its wide application in industry. A large number of correlations for saturated flow boiling inside horizontal and vertical tubes are available in the literature (Kandlikar, 1990; Sumith et al., 2003).

☆ This paper is dedicated to Professor George Yadigaroglu, on the occasion of his 65th birthday. George is a close and dear friend of the "corresponding author" for many years. We have taught a course together for some 24 years, and must have signed 1300 certificates for the participants. We also edited this journal for many years, until he decided that he had enough. But most of all we like to spend time on "his" island in Greece, where the food is good, and his olive trees are green. Thanks for all these.

* Corresponding author. Tel.: +972-48-292058; fax: +972-48-238-101.
E-mail address: hetsroni@techunix.technion.ac.il (G. Hetsroni).

0301-9322/$ - see front matter © 2004 Elsevier Ltd. All rights reserved.
doi:10.1016/j.ijmultiphaseflow.2004.05.001

Only a few studies of saturated boiling were conducted in annular channels. Early visualization experiments carried out by Hewitt et al. (1965) showed that the bubbles affect the nucleation activity. The presence of moving bubbles leads to the wave-induced nucleation phenomenon observed by Barbosa et al. (2003). It was suggested that the heat transfer coefficient should increase in the wave region, though in the study of Barbosa et al. (2003) there were no direct measurements to confirm this conclusion.

In the wave region, a thick film of liquid occurs on the heated inner tube, which would imply a considerable decrease in the heat transfer coefficient and a consequent increase in the wall temperature. Barbosa et al. (2002) conducted experiments in a vertical annulus in which heat was applied to the inner surface of the channel. A dominance of nucleate boiling was observed at low qualities (generally lower than a few per cent). At high qualities, nucleate boiling was partly or totally suppressed and forced convection became the dominant mechanism. Thus, one may conclude that in internal flow boiling, the heat transfer coefficient is a combination of two mechanisms, nucleate boiling and forced convection.

The heat transfer coefficient might remain constant, decrease or increase depending on the contribution of these two mechanisms during forced saturation boiling. It was shown by Hetsroni et al. (2001b, 2002a) that addition of a small amount of surfactant significantly decreased the bubble size. Under these conditions the heat transfer coefficient increases in saturated boiling of surfactants compared to that in pure water.

Heat exchangers with small channels are prevalent in industries such as electronic, transport, and chemical processing. The surface tension force is important and might affect flow patterns and heat transfer in such channels. However, only a few studies have tried to clarify the effect of the gap size of an annular channel on heat transfer. Fukano et al. (2002) made a detailed investigation of the wall temperature near a cylindrical spacer in the case where repeating dryout and rewetting occurred on the heating surface. Recently Fukano et al. (2003) and Mori and Fukano (2003) clarified the influence of an obstacle on heat transfer with stepwise changes of such parameters as heat flux, mass flow rate, and quality at the test section inlet. It was shown that transient burnout was possible even when the operating conditions after the change, were less than the steady burnout condition. No studies of this phenomenon were found for surfactant solutions.

In the present study, the working fluids were water and a surfactant solution that is benign in terms of environmental impact. Specifically, saturated flow boiling at low values of mass fluxes was studied because it helps to understand the process in compact heat exchangers.

2. Experimental apparatus and procedure

2.1. Experimental apparatus

Fig. 1 is a schematic view of the experimental apparatus. The pump (2) delivered the fluid to the inlet manifold of the test section from the inlet tank (1), where the fluid temperature was maintained by a thermostat. The flow rate of the working fluid was controlled by a valve (3) and measured by a rotameter (4). The steam–water mixture generated in the annular channel of the test section was directed through the outlet manifold to the outlet tank (8). The local temperatures

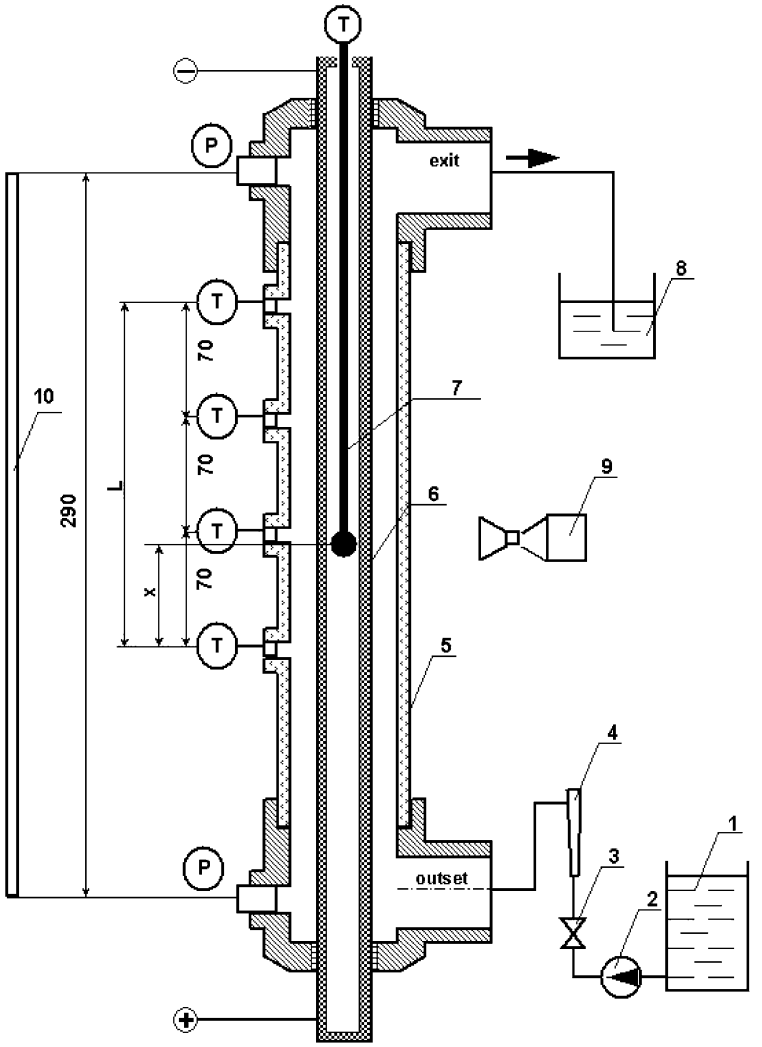

Fig. 1. Experimental apparatus: (1) inlet tank, (2) pump, (3) valve, (4) rotameter, (5) glass tube, (6) heated tube, (7) thermocouple, (8) outlet tank, (9) video system, and (10) ruler.

of the fluid, which passed through the test section, were measured by thermocouples, inserted into the annulus. Experiments were performed at atmospheric pressure. Heat transfer data were taken as the heat flux was increased, as well as with heat flux being decreased step by step.

The test section consisted of a central stainless steel tube (6) with an inner diameter $d_1 = 2.2$ mm, an outer diameter $d_2 = 3.2$ mm and length $L = 290$ mm. The ends of the tube were soldered to power supply electrodes. The tube was heated by DC current. The temperature on the heated wall of the test section was measured by a radiation equilibrium thermocouple (7) that can be moved along the tube (6). The annulus was formed between the heated tube (6) and unheated glass tube (5) of inner diameter 12 mm and outer diameter 17 mm. The pressure readings were

taken from pressure taps (P) at the inlet and the outlet of the test section. Absolute pressures were measured by pressure transducers. The saturation temperature at a given point in the test section was calculated through a linear interpolation between the values of the saturation temperatures corresponding to the pressure readings. The temperature on the outer wall of the glass tube was measured by thermocouples to estimate the heat losses.

Direct observation of the flow was carried out by using a high-speed video recording system (9) with recording rate up to 10,000 frames per second. The playback speed could be varied from a single frame to 250 frames per second. For the runs in which visualization of the boiling process was carried out, the camera was mounted on a tripod and directed at the heated portion of the test section. The field of view was of the order 30 mm × 30 mm. A ruler (10) was used to measure the distance from the outset.

2.2. Properties of surfactant solution

We used Alkyl (8–16) Glycoside, a nonionic surfactant solution of molecular weight 390 g/mol. The measurements of surface tension were carried out for different concentrations of surfactant solutions over a range of temperature from 300 to 368 K. In Fig. 2 the equilibrium surface tension, σ, is plotted vs. the concentration of the surfactant solution at different temperatures. An increase in the surfactant concentration up to $C = 300$ ppm (parts per million weight) leads to significant decrease in surface tension. The surface tension was almost independent of concentration in the range $300 \leqslant C \leqslant 1200$ ppm. In all cases an increase in liquid temperature leads to a decrease in surface tension. In the present study, a concentration of $C = 300$ ppm was used. The solution was prepared by dissolving the surfactant (52% active substance and 48% water) in deionized water, with gentle stirring over a period of a day.

2.3. Error analysis

Electrical power was determined with an accuracy of 0.5%. The surface heat flux was calculated by measuring the power delivered to the heated inner surface and by determination of heat losses.

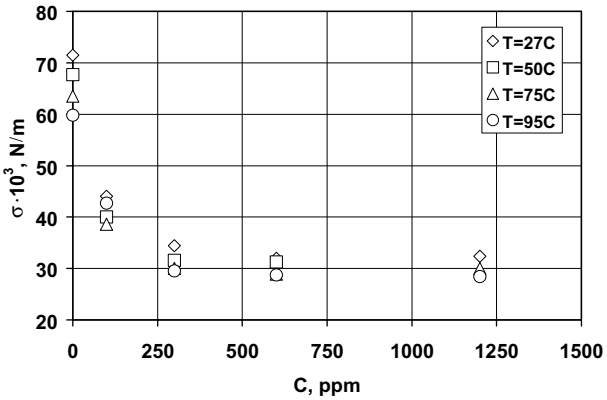

Fig. 2. Surface tension of Alkyl (8–16) Glucoside solution vs. concentration at different temperatures.

Table 1
Uncertainty of the measurements

Item	Designation	Bias limit B	Precision limit P (%)
Heat flux	q	1 k W/m^2	2.0
Wall temperature	T_w	0.3 K	1.0
Bulk temperature	T_f	0.5 K	2.0
Saturation temperature	T_s	0.1 K	0.2
Mass flow rate	m	0.04 kg/m^2 s	2.0
Location along the heater	x	0.5 mm	5

The temperature of the heated surface and of the working fluid was measured by 0.3 mm type-T thermocouples. The thermocouples and the data acquisition system were calibrated at steam point and ambient water temperature, and yield values within 0.3 K at these two conditions. The rotameter was calibrated at its operating temperatures with an accuracy of 1%. The estimated accuracy in the calculation of the saturation temperature is 0.1 K. The error associated with the measurement of the distances between the thermocouple locations is 0.5 mm. In order to calculate the deviations associated with the measurement of various quantities, readings were taken for a few sample runs every 2 min over a period of 20 min. The uncertainty analysis was performed according to the ASME Policy on Reporting Uncertainties in Experimental Measurements and Results. The results of the uncertainty analysis are given in Table 1, where the bias limit is an estimate of the magnitude of the fixed constant error. The precision limit is an estimate of the lack of repeatability caused by random errors and unsteadiness. The uncertainty in the heat transfer coefficient with 95% confidence interval is between 9% and 16%. The uncertainty is higher at the higher values of heat transfer coefficient due to the small temperature difference between the wall and the fluid. Error bars are shown in the figures on which experimental results are presented.

2.4. Verification of the method

A number of verification runs were performed prior to data logging. It was assumed that under the condition of saturated boiling of water the heat transfer was not dependent on mass flow rate, since the mass flux was small in the present study. The saturated boiling data in our annular channel were compared to the measurements conducted in narrow space by Fujita et al. (1988). In that study, experiments on heat transfer characteristics in pool boiling were performed in a confined space bounded by a rectangular heating surface and an opposed unheated plate. Various parameters, which may affect the boiling heat transfer, were taken into account. They were the gap size and the length of the gap. We compared our data for length of heating surface, 210 mm, to those presented by Fujita et al. (1988) for gap size of 5 mm, closed side periphery, and the length of the heating surface of 120 mm. Their gap size is close to the hydraulic radius of the test section, $r_h = 4.4$ mm, used in the present study. It can be seen from Fig. 3 that the agreement is good for the results obtained in an annular channel and the data of Fujita et al. (1988).

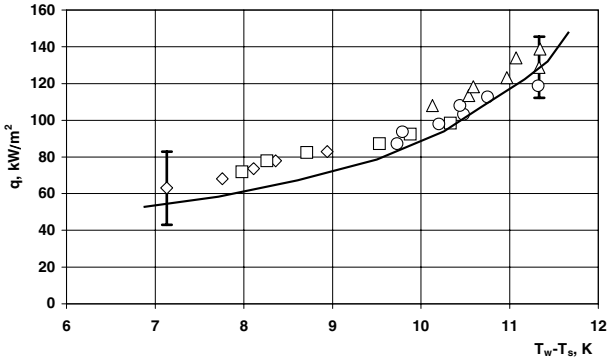

Fig. 3. Boiling curve of water flow in the annular channel: (◇) $\dot{m} = 3.2$ kg/m^2 s, (□) $\dot{m} = 4.6$ kg/m^2 s, (○) $\dot{m} = 5.7$ kg/m^2 s, (△) $\dot{m} = 6.6$ kg/m^2 s, (—) the data of Fujita et al. (1988).

2.5. Experimental runs

First, the liquid flow rate and the temperature at the inlet of the test section were adjusted. After that the electrical power to the heater was gradually increased. For each value of heat flux, when steady state was attained, the wall temperature was measured at various distances along the heater. It was assumed that steady state was reached when the thermocouple reading at the given position was steady. Experiments were conducted under conditions at heat fluxes lower than CHF. Thus, at given value of fluid inlet temperature and flow rate, the maximum operating heat flux did not exceed the value at which the heating surface temperature would rise suddenly. Afterwards, electrical power was gradually decreased and measurements were conducted under conditions of decreasing heat flux.

A fresh sample of surfactant solution was used after three runs to minimize changes in solution properties, which might have occurred at high temperature due to evaporation. No visible deposits formed under the test conditions, based on observations in the test runs and after draining the test section. The ranges of experimental conditions are given in Table 2 for both surfactant solution and pure water.

The heat flux was determined as

$$q_w = (N - N_{loss})/\pi d_2 L, \tag{1}$$

where N is the electrical power, N_{loss} are heat losses to the environment, d_2 is the outer diameter of the heated tube, L is the heated length.

The local heat transfer coefficient, α, in the saturated boiling region was calculated by

$$\alpha = q_w/(T_w - T_s), \tag{2}$$

Table 2
The principal operating characteristics of the experiments

Inlet temperature, T_0 (K)	Mass flux, m (kg/m^2 s)	Heat flux, q (kW/m^2)	Vapor quality, X (%)
303	3.2–6.6	50–140	5–16
338	5.7–7.7	70–140	6–28

where q_w is the heat flux, T_w, and T_s are the local wall temperature and saturation temperature, respectively.

The local wall temperature T_w is the temperature of the outer surface of the heated section. It may be determined by measuring the temperature of the inner surface of the thin-walled heater, using a sliding thermocouple (Hetsroni et al., 2001b, 2002b; Barbosa et al., 2002). The tip of the thermocouple is placed on the axis of the heated tube. The thermocouple measures the temperature of the inner tube wall because inside of the tube $\operatorname{grad} T = 0$ if the effect due to free convection within the airspace into the tube is negligible. The thermocouple tip does not touch the tube. The measurements are based on radiation equilibrium between the inner tube surface and the tip.

The temperature of the outer heater wall, T_w, can be estimated by solving a steady-state heat conduction equation

$$dT/dr = -q_v/k, \tag{3}$$

where q_v is the volumetric heat generation rate in the heater and k is the thermal conductivity of the heater. Eq. (3) can be integrated with the following boundary condition,

$$T = T_{w,1} \text{ at } r = r_1.$$

The resultant equation is

$$T_w = T_{w,1} - \frac{q_w \cdot r_1^2}{4k}\left[\left(\frac{r_2}{r_1}\right)^2 - 2\ln\frac{r_2}{r_1} - 1\right]. \tag{4}$$

The average heat transfer coefficient, α_{av}, was calculated as

$$\alpha_{av} = \frac{1}{L}\int_0^L \alpha\, dL. \tag{5}$$

3. Results

3.1. Flow pattern

3.1.1. Flow visualization

Fig. 4a–f and g–l show regimes of boiling along different parts of the test section for water and 300 ppm solution of surfactant, respectively. The direction of the flow is from the bottom to the top, the heat flux is $q = 90$ kW/m^2, the mass flux is $\dot{m} = 5.7$ kg/m^2 s and the inlet flow temperature is $T_0 = 338$ K. In these figures the inner heated tube appears as a dark vertical cylinder in the middle of the picture. The ruler is also shown in these figures for reference.

3.1.2. Onset of nucleate boiling (ONB)

The first bubbles appear on the wall at a location, which is identified as the onset of nucleate boiling. ONB occurs when the wall temperature exceeds the saturation temperature by a certain amount, and bubbles begin to nucleate on the heated surface. From Fig. 4a and g one can see that under the conditions of the present experiment, the first bubbles appeared at the same distance

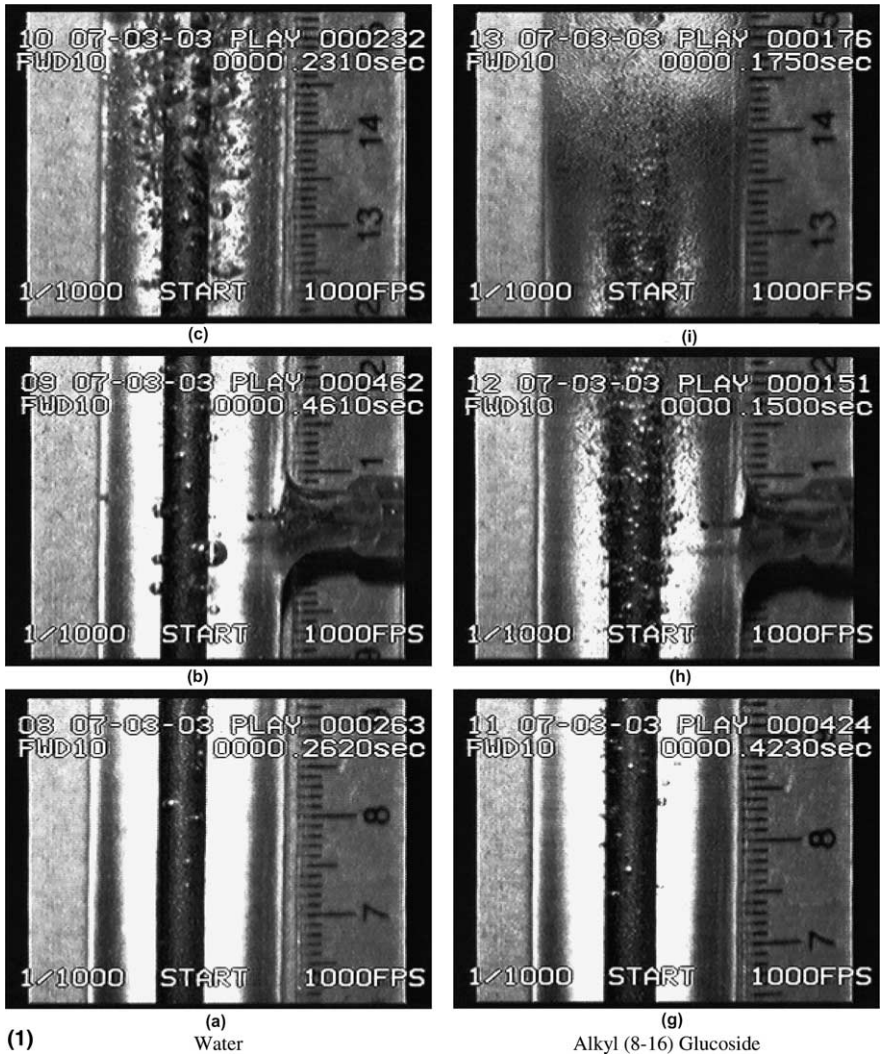

Fig. 4. Visualization of flow boiling regions: (1) subcooled boiling and OSB; (2) saturated boiling $T_0 = 338$ K, $\dot{m} = 5.7$ kg/m^2 s, $q = 90$ kW/m^2; (a–f) water flow; (g–l) flow of surfactant solution.

from the inlet for both fluids: water and 300 ppm surfactant solution. The ONB level corresponds to about 7.5 cm on the ruler.

3.1.3. Subcooled boiling

This region is shown in Fig. 4b and h for water and surfactant, respectively. The phenomenon, which is presented in Fig. 4b, illustrates typical behavior observed in the current study for water flow. In the region, which starts right after the ONB, bubbles slide long distances on the heater before eventually being ejected into the liquid. The explosive bubble growth soon after nucleation, is later replaced by balanced evaporation and condensation rates leaving bubbles with fairly

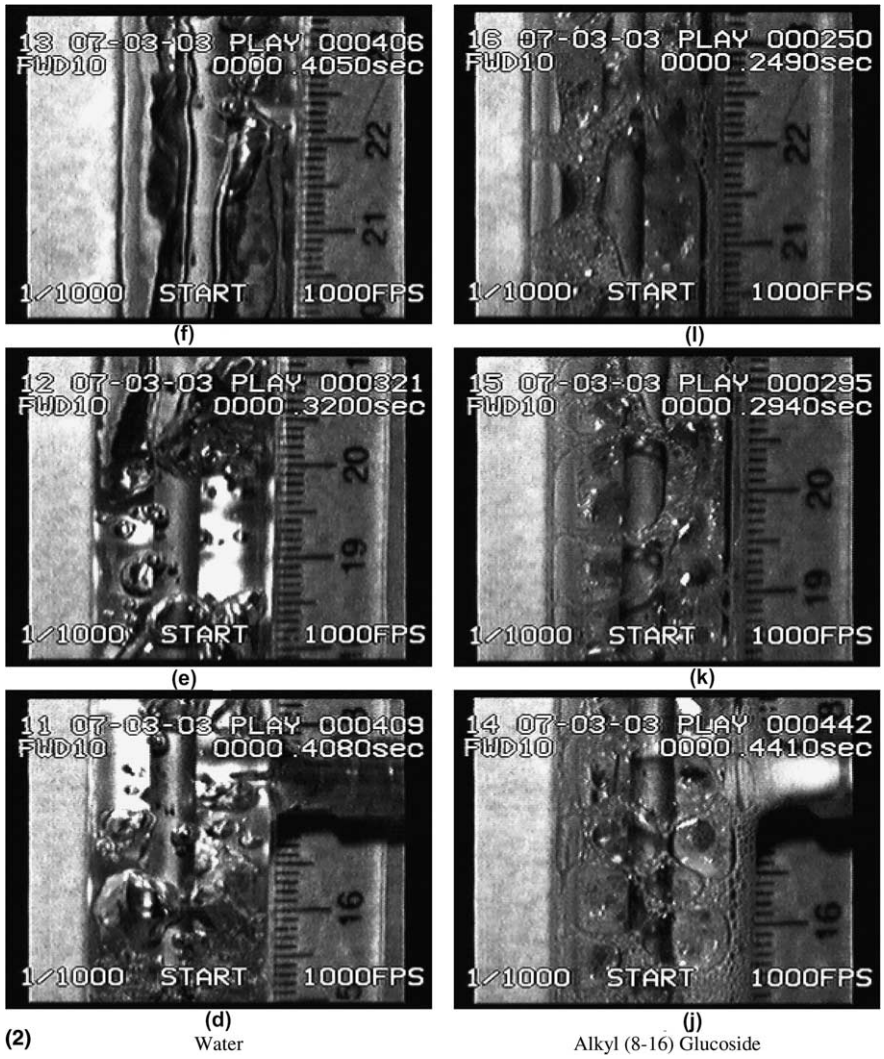

Fig. 4 (*continued*)

constant size and shape for a significant amount of time. Prodanovic et al. (2002) discussed in details this type of bubble behavior. For surfactant solution flow the bubble behavior in this region is shown in Fig. 4h. More active nucleation sites were observed in this region compared to water flow.

3.1.4. Onset of saturation boiling, OSB

As heat addition continues downstream, the thermodynamic equilibrium saturation is reached at a distance, x_0, from the entrance of the test section. This point is identified as the onset of saturated flow boiling, or OSB. Heat transfer beyond OSB is the main focus of the present study. In this region the complex interactions between the liquid film close to the heater and the bubbles

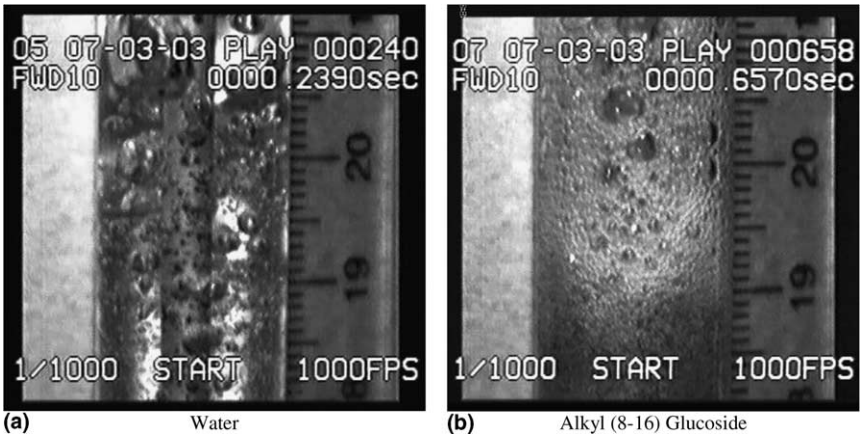

Fig. 5. Saturated boiling $T_0 = 338$ K, $\dot{m} = 5.7$ kg/m^2 s, $q = 60$ kW/m^2: (a) water flow; (b) flow of surfactant solution.

in the bulk flow take place. In this case, the bulk fluid temperature $T_f = T_s$. From flow visualization the experimental evidence of OSB is characterized by the end of condensing bubbles and the bubbles start to fill the whole cross-section of the annular channel. Fig. 4c and i show that the location of OSB, x_0, is the same distance from the outset (about 14 cm on the ruler) for both fluids: water and 300 ppm surfactant solution.

The location of the onset of saturation boiling, x_0, can be also defined by an energy balance:

$$qd_1x_0 = \frac{1}{4}\dot{m}c_p(T_s - T_0)(d_3^2 - d_2^2), \tag{6}$$

where T_s is the saturation temperature, T_0 is the fluid temperature at the inlet to the test section, $\dot{m}$ is the mass flux and d_3 is the inner diameter of the glass tube.

A small amount of surfactant does not change the specific heat, c_p, of the solution compared to pure water. Thus, for both water and surfactant solution, the onset of saturation boiling occurs at the same distance from the inlet.

3.1.5. Saturated boiling along the heated surface

Fig. 4d–f present a sequence of pictures of water flow after OSB. An increase in the distance from OSB leads to a region of nucleate boiling, in which the bubbles are pushed away from the wall, Fig. 4d and e. On the upper part of the channel, Fig. 4f, most of the heating surface was steadily covered with vapor and a wavy liquid–vapor interface was observed in the moving video sequences. Developed nucleate boiling of surfactant solution is presented in Fig. 4j–l in which small bubbles flowed mainly in the longitudinal direction. The moving video sequences showed that these bubbles appeared more frequently than those in water flow. Such behavior leads to increased heat transfer coefficients in the region of saturated flow boiling of surfactant solution compared to water.

The effect of heat flux on saturated flow boiling is shown in Fig. 5a and b. These figures were obtained under the same flow condition as Fig. 4e and k but the heat flux was $q = 60$ kW/m^2.

3.2. Temperature distribution along the channel

In this section we consider temperature measurements on the heater surface, T_w, and the heat transfer coefficient, α, at different locations from the inlet to the location of the measurements, x. The results are presented for the regime of saturated flow boiling, i.e. for the dimensionless distance $x/x_0 \geqslant 1$. The location of OSB, x_0, was obtained from Eq. (4).

3.2.1. Local heat transfer coefficient

Fig. 6a and b depict the dependence of T_w, and of α_w on the dimensionless length, x/x_0, for flow boiling of water. The experimental conditions were: the inlet temperature $T_0 = 338$ K, mass flux $\dot{m} = 5.7$ kg/m^2 s, heat flux $q = 90$ kW/m^2. Fig. 7a and b depict the dependence of T_w, and of α_s on the dimensionless length, x/x_0, for flow boiling of surfactant solution at the same experimental conditions. Comparison of these figures shows that the heat transfer coefficients for surfactant solution, α_s, are much higher than those for pure water, α_w.

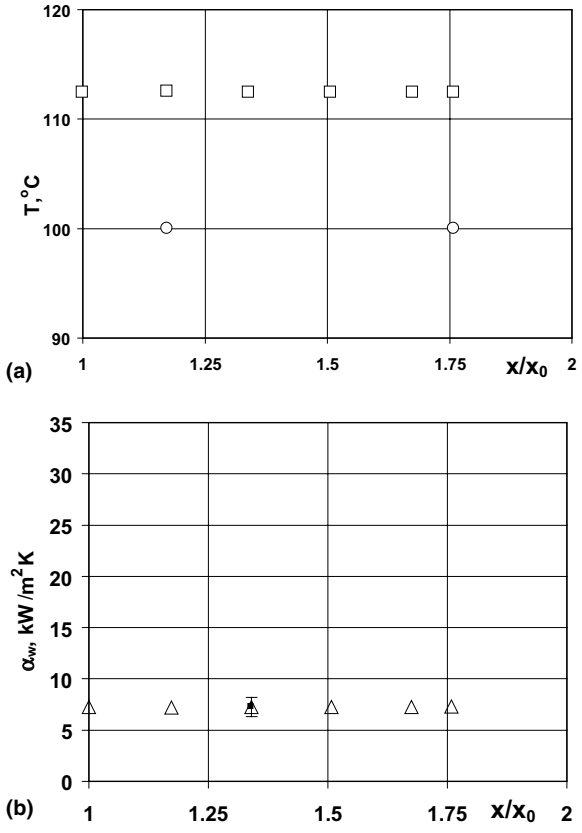

Fig. 6. Temperature of the heater and local heat transfer coefficient of saturated flow boiling of water $T_0 = 338$ K, $\dot{m} = 5.7$ kg/m^2 s, $q = 90$ kW/m^2: (a) temperature distribution, (b) heat transfer coefficient; (□) T_w, (○) T_s, (△) α_w.

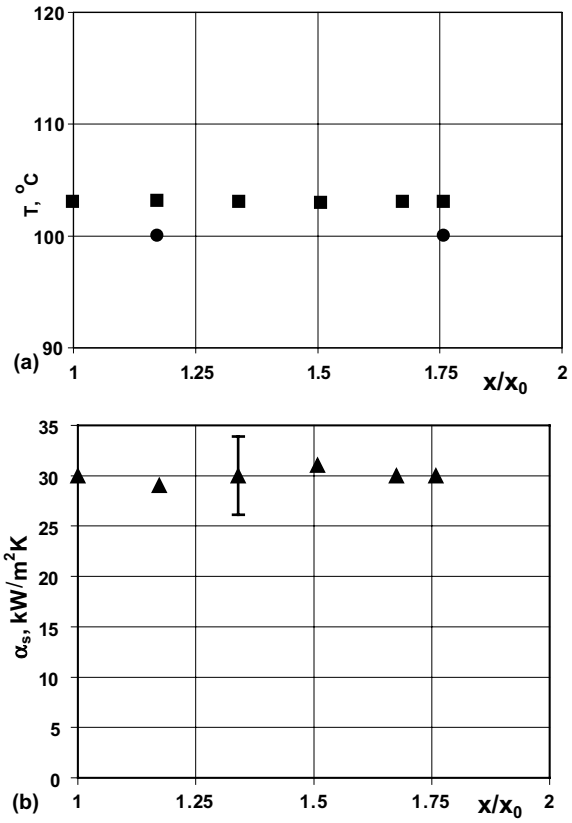

Fig. 7. Temperature of the heater and local heat transfer coefficient of saturated flow boiling of surfactant solution $T_0 = 338$ K, $\dot{m} = 5.7$ kg/m^2 s, $q = 90$ kW/m^2: (a) temperature distribution, (b) heat transfer coefficient; (■) T_w, (●) T_s, (▲) α_s.

3.2.2. *Effect of heat flux*

At given value of mass flux the ONB location depends on the heat flux. Even a small increase in heat flux might lead to the transition of the dominant heat transfer mechanism from nucleate boiling to thin liquid evaporation or to film evaporation with partial dryout. The flow regime transition affects behavior of the local heat transfer coefficient.

Fig. 8a and b depict the dependence of T_w, and α_w on the dimensionless length, x/x_0, for saturated flow boiling of water. The experimental conditions were: inlet temperature $T_0 = 338$ K, mass flux $\dot{m} = 5.7$ kg/m^2 s, heat flux $q = 110$ kW/m^2. From Figs. 8b and 6b one can conclude that a small increase in heat flux from $q = 90$ kW/m^2 to $q = 110$ kW/m^2 had little effect on the heat transfer coefficient.

Fig. 9a and b depict the dependence of T_w, and of α_w on the dimensionless length, x/x_0, for flow boiling of surfactant solution at experimental conditions: inlet temperature $T_0 = 338$ K, mass flux $\dot{m} = 5.7$ kg/m^2 s, heat flux $q = 110$ kW/m^2. From comparing Figs. 9b and 7b it is clear that the heat transfer coefficient obtained at $q = 110$ kW/m^2 is lower than that obtained at $q = 90$ kW/m^2. Fig. 9b shows that the heat transfer coefficient decreases along the heated surface due to the beginning of departure from nucleate boiling, DNB.

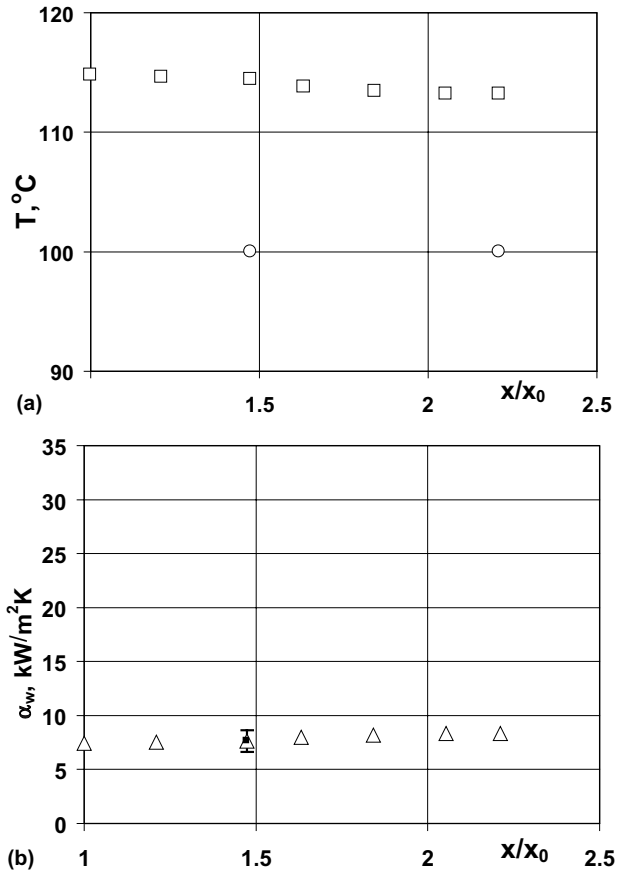

Fig. 8. The effect of heat flux on heat transfer in water flow $T_0 = 338$ K, $\dot{m} = 5.7$ kg/m^2 s, $q = 110$ kW/m^2: (a) temperature distribution, (b) heat transfer coefficient; (□) T_w, (○) T_s, (△) α_w.

3.2.3. *Effect of length of the heating surface*

Subcooling and mass flux of surfactant solution significantly affect the local heat transfer coefficient. According to Eq. (6) the OSB point, x_0, shifts along the heated surface depending on these parameters. On the other hand, under condition of saturated boiling the thermodynamic equilibrium quality, X, may be calculated by applying the heat balance equation over the heated length between the inlet section and the thermocouple location. Such properties as density and specific heat of 300 ppm concentration of surfactant solution do not differ from those of the solvent. At the same thermocouple location and the same heat flux the thermodynamic equilibrium quality is the same for pure water and surfactant solution. Thus, the quality cannot explain the difference between the boiling of water and of surfactant solution. Surfactant additives tend to appreciably change the boiling curve due to modifying nucleation and bubble dynamics. Therefore we present the local heat transfer coefficient data dependence on the dimensionless coordinate, x/x_0.

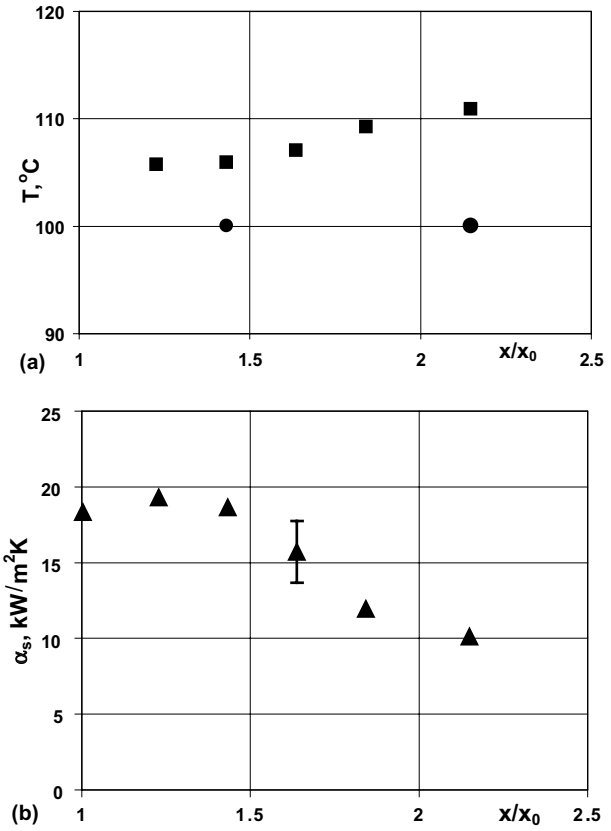

Fig. 9. The effect of heat flux on heat transfer in flow of surfactant solution $T_0 = 338$ K, $m = 5.7$ kg/m^2 s, $q = 110$ kW/m^2: (a) temperature distribution, (b) heat transfer coefficient; (■) T_w, (●) T_s, (▲) α_s.

3.3. Boiling curves

We consider boiling curves obtained at a distance $L = 210$ mm. The experimental data of saturated boiling of surfactant solution differ from the usual boiling curve. The boiling curves for surfactant solution demonstrate unusual behavior, i.e. at low heat flux the temperature of the heated wall decreases with an increase in the heat flux and $dq/dT_w < 0$. At high values of heat flux, the temperature of the heated wall increases with an increase in heat flux and $dq/dT_w > 0$. A typical boiling curve, obtained under conditions $\dot{m} = 3.2$ kg/m^2 s, $T_0 = 303$ K is presented in Fig. 10. The measurements were repeated several times and the same phenomenon was observed. Point A reflects the condition, at which the wall temperature starts to decrease with an increase in heat flux. Point B indicates the minimum superheat detected in the test. The curve AB corresponds to $dq/dT_w < 0$, the curve BC corresponds to $dq/dT_w > 0$. The generation of the bubble in the liquid film becomes more vigorous with an increase in heat flux. Then the temperature difference $T_w - T_s$ becomes smaller with an increase in heat flux as AB line. It should be stressed that the boiling curve is not a boiling hysteresis.

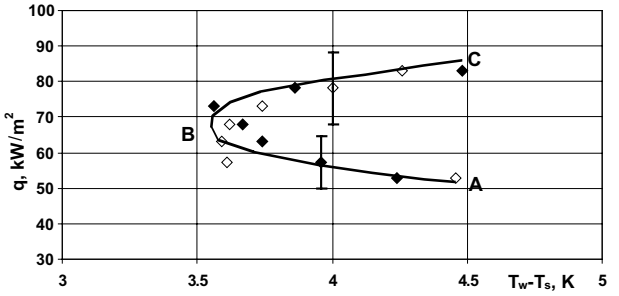

Fig. 10. The effect of the heat flux direction on boiling curve of surfactant solution $T_0 = 303$ K, $\dot{m} = 3.2$ kg/m^2 s: (◆) increase in heat flux, (◇) decrease in heat flux.

Boiling curves for which $dq/dT_w < 0$, were not observed for saturated flow boiling of pure water, since the size of the bubble was larger than that for boiling of surfactant solution. It was shown by Kurose and Komori (1999) and Hetsroni et al. (2001a, 2002b) that an increase in bubble diameter may lead to a negative value of the lift coefficient, i.e. the lift force acts from the higher-fluid-velocity side to the lower-fluid-velocity side. The negative lift force together with the friction causes increase in waiting period and wall temperature increases with an increase in the heat flux even at low values of heat flux. Behavior of the boiling curve, at which $dq/dT_w < 0$, was also not observed for subcooled pool boiling of surfactants (Hetsroni et al., 2002a) since in this case the shear flow did not exist.

Fig. 11 shows the effect of mass flux on the boiling behavior at $T_0 = 303$ K. From this figure one can conclude that the boiling curve shifts to higher values of wall superheat with an increase in mass flux.

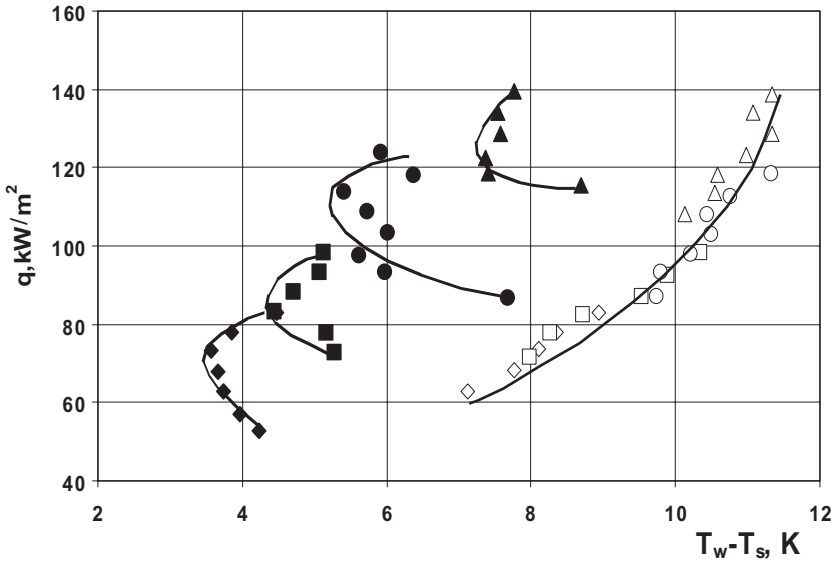

Fig. 11. The effect of the mass flux on boiling curve of surfactant solution $T_0 = 303$ K: (◆) $\dot{m} = 3.2$ kg/m^2 s, (■) $\dot{m} = 4.6$ kg/m^2 s, (●) $\dot{m} = 5.7$ kg/m^2 s, (▲) $\dot{m} = 6.6$ kg/m^2 s, (—) water flow.

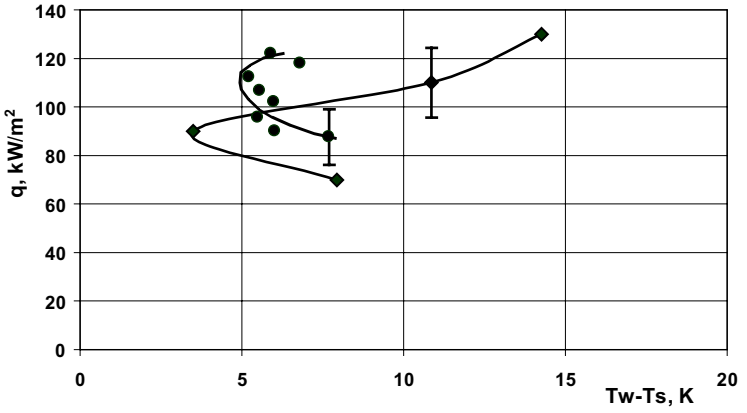

Fig. 12. The effect of the inlet temperature on the boiling curve of surfactant solution $\dot{m} = 5.7$ kg/m^2 s: (◆) $T_0 = 303$ K, (●) $T_0 = 338$ K.

The effect of the inlet temperature is illustrated in Fig. 12 for mass flux of $\dot{m} = 5.7$ kg/m^2 s and inlet temperature of $T_0 = 338$ K. Figs. 11 and 12 demonstrate that saturated flow boiling of 300 ppm Alkyl (8–16) Glucoside solution cannot be described by a common boiling curve.

The effect of heat flux is illustrated in Fig. 5a and b and in Fig. 4e and k. From Fig. 5a and b one can conclude that at $q = 60$ kW/m^2, for both water and surfactant solution, flow nucleate boiling took place. The presence of surfactant in the cavities initiates the nucleus formation. High-speed visualization showed that the bubbles eventually emerge and are spherical in shape. Photographic evidence revealed that the bubbles associated with the surfactant solution were generally smaller and more numerous than in the water flow boiling experiments. This effect leads to an increase in the heat transfer coefficient and is more pronounced with an increase in heat flux. Fig. 4e and k show that an increase in heat flux up to a value of $q = 90$ kW/m^2 changed the flow pattern and enhanced two-phase structures were observed. Liquid film was generated frequently and the film thickness fluctuated due to alternate passing of liquid lumps and large vapor bubbles, with a decrease in heat transfer. For flow of surfactant solution heat transfer is higher than that for water since the disturbance waves pass the heater more frequently.

3.4. Average heat transfer coefficient

The effect of the surfactant on boiling heat transfer can be presented as a relation of the average heat transfer coefficient, over the whole region of saturated flow boiling, in surfactant solution, α_{avs}, to that in pure water, α_{avw}.

Fig. 13 shows the dependence of $\alpha_{avs}/\alpha_{avw}$ on the heat flux for inlet temperature $T_0 = 338$ K and two values of mass flux: $\dot{m} = 5.7$ kg/m^2 s and $\dot{m} = 7.7$ kg/m^2 s. The relative heat transfer coefficient increases with an increase in the heat flux and reaches a maximum of about four. At higher values of heat flux the decrease in the plot is due to a departure from nucleation boiling regime. It should be noted that the dashed line qualitatively described the experimental data, since no tests were conducted at heat fluxes close to $q = 90$ kW/m^2.

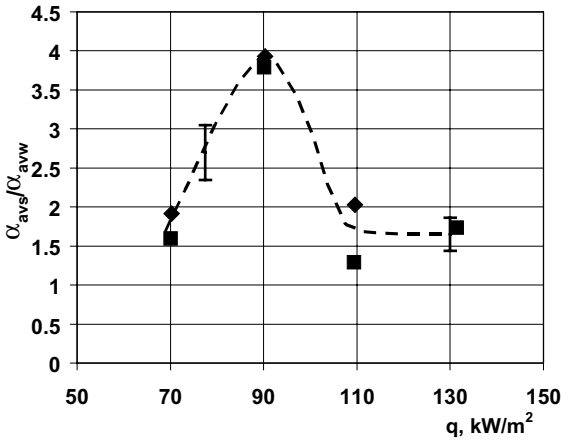

Fig. 13. The relative heat transfer coefficient $T_0 = 338$ K: (◆) $\dot{m} = 5.7$ kg/m^2 s, (■) $\dot{m} = 7.7$ kg/m^2 s.

4. Conclusions

The location of the beginning of saturated boiling, OSB, is the same at equal values of mass flux, heat flux and inlet temperature for the flow boiling of pure water and of surfactant solution in an annular channel.

The average heat transfer coefficient of the surfactant solution may be up to four times higher than that of pure water in the saturated flow boiling region. The increase in the heat transfer coefficient depends on the heat flux. At a high value of heat flux the heat transfer coefficient decreases due to departure from the nucleate boiling regime.

Boiling curves for surfactant solution demonstrate unusual behavior, i.e. at low heat flux the temperature of the heated wall decreases with an increase in heat flux.

Acknowledgements

This research was supported by a Grant from the G.I.F., the German–Israeli Foundation for Scientific Research and Development. A. Mosyak and R. Rozenblit were supported by a joint grant from the Center for Absorption in Science of the Ministry of Immigrant Absorption and the Committee for Planning and Budgeting of the Council for Higher Education under the framework of the Kamea Program, and E. Pogrebnyak was supported by the Center for Absorption in Science, Ministry of Immigrant Absorption State of Israel. The authors are indebted to Jeffrey Ellis who performed the surface tension measurements at Ohio State University.

References

Barbosa, J.R., Hewitt, G.F., Richardson, S.M., 2002. Forced convective boiling of steam–water in a vertical annulus at high qualities. Exp. Therm. Fluid Sci. 26, 65–75.

Barbosa, J.R., Hewitt, G.F., Richardson, S.M., 2003. High-speed visualization of nucleate boiling in a vertical annular flow. Int. J. Heat Mass Transfer 46, 5153–5160.

Fujita, Y., Ohta, H., Uchida, S., Nishikawa, K., 1988. Nucleate boiling heat transfer and critical heat flux in narrow space between rectangular surfaces. Int. J. Heat Mass Transfer 31, 229–239.

Fukano, T., Mori, S., Akamatsu, S., Baba, A., 2002. Relation between temperature fluctuation of a heating surface and generation of drypatch caused by a cylindrical spacer in a vertical boiling two-phase upward flow in a narrow annular channel. Nucl. Eng. Des. 217, 81–90.

Fukano, T., Mori, S., Nakagawa, T., 2003. Fluctuation characteristics of heating surface temperature near an obstacle in transient boiling two-phase flow in a vertical annular channel. Nucl. Eng. Des. 219, 47–60.

Hetsroni, G., Li, C.F., Mosyak, A., Tiselj, I., 2001a. Heat transfer and thermal pattern around a sphere in a turbulent boundary layer. Int. J. Multiphase Flow 27, 1127–1150.

Hetsroni, G., Zakin, J.L., Lin, Z., Mosyak, A., Pancallo, E.A., Rozenblit, R., 2001b. The effect of surfactants on bubble growth, wall thermal patterns and heat transfer in pool boiling. Int. J. Heat Mass Transfer 44, 485–497.

Hetsroni, G., Gurevich, M., Mosyak, A., Rozenblit, R., Yarin, L.P., 2002a. Subcooled boiling of surfactant solutions. Int. J. Multiphase Flow 28, 347–361.

Hetsroni, G., Mosyak, A., Pogrebnyak, E., 2002b. Effect of coarse particles on heat transfer in a particle-laden turbulent boundary layer. Int. J. Multiphase Flow 28, 1873–1894.

Hewitt, G.F., Kersey, H.A., Lacey, P.M.C., Pulling, D.J., 1965. Burnout and nucleation in climbing film flow. Int. J. Heat Mass Transfer 8, 793–814.

Kandlikar, S.G., 1990. A general correlation for saturated two-phase flow boiling heat transfer inside horizontal and vertical tubes. J. of Heat Transfer 112, 219–228.

Kurose, R., Komori, S., 1999. Drag and lift forces on a rotating sphere in a linear shear flow. J. Fluid Mech. 384, 183–206.

Mori, S., Fukano, T., 2003. Influence of a flow obstacle on the occurrence of burnout in boiling two-phase upward flow within a vertical annular channel. Nucl. Eng. Des. 225, 49–63.

Prodanovic, V., Fraser, D., Salcudean, M., 2002. On the transition from partial to fully developed subcooled flow boiling. Int. J. Heat Mass Transfer 45, 4727–4738.

Sumith, B., Kaminaga, F., Matsumara, K., 2003. Saturated flow boiling of water in a vertical small diameter tube. Exp. Therm. Fluid Sci. 27, 789–801.